Lithuanian Journal of Physics, Vol. **45**, No. 2, pp. 133–137 (2005)

# NONLINEAR $I$–$V$ CHARACTERISTICS IN POLYANILINE DUE TO PHONON-ASSISTED TUNNELLING

A. Kiveris and P. Pipinys

*Department of Physics, Vilnius Pedagogical University, Studentų 39, LT- 08106 Vilnius, Lithuania*
E-mail: studsk@vpu.lt

Received 11 April 2005

Non-linear temperature-dependent current–voltage ($I$–$V$) characteristics of an organic polyaniline (PAN) thin films diodes measured by Kieffel et al. (Synth. Met. **135–136**, 325–326 (2003)) is explained on the basis of phonon-assisted tunnelling initiated by electrical field. The results of temperature dependence of conductivity in PAN films presented in references: Gosh et al., Phys. Lett. A **260**, 138–148 (1999), Mzenda et al., Synth. Met. **127**, 285–289 (2002), and Maser et al., Mater. Sci. Engin. C **23**, 87–91 (2003) are also explained on the basis of the free charge carrier generation tunnelling mechanism. From the fit of the experimental data with the present model the density of localised states which take part in the current flow is estimated.

**Keywords:** polyaniline, current–voltage characteristics, phonon-assisted tunnelling

**PACS:** 72.10.Di, 73.61.Ph, 73.40.Gk

## 1. Introduction

The conducting polyaniline polymers have received widespread applications because they are soluble, have variable conductivity, and can be easily processed in both doped and undoped forms [1, 2]. To understand the electronic transport properties of PAN, a number of studies on conductivity have been performed in the last few years [1–8]. Experimental measurements reveal that electrical conduction in PAN (undoped or lightly doped) is temperature-activated and decreases by several orders of magnitude as the temperature is lowered [4].

In Refs. [4, 5] the charge transport has been described as a superposition of different conduction phenomena, because the morphology of PAN comprises metallic islands surrounded by amorphous regions. In charge transport, metallic conduction takes place in metallic regions, and charge hops in amorphous regions.

Pelster et al. [6] have suggested that the electronic transport in the PAN is governed by the three-dimensional (3D) hopping between these crystalline regions, an average size of which has been estimated to be about 8 nm, surrounded by amorphous polyaniline. Gosh et al. [1] have observed that the electrical conductivity of HCl-doped conducting PAN increases with increasing the temperature and that the variation is remarkably high at higher temperature, whereas at low temperature the conductivity variation is very small. The authors of Ref. [1] have ascribed the high temperature (10 K$\leq T\leq$260 K) conductivity to the Mott's ($\exp(T^{-1/4})$) variable range hopping among the localized states. The temperature-dependent conductivity at low temperatures ($T$<10 K) has been described by the relation $\sigma(T) \propto \exp[-(T_0/T)^{1/2}]$, where $T_0$ is the characteristic temperature.

The observed variation of the activation energy with temperature, in the opinion of the authors of [1], suggests that the band conduction model is not sufficient to explain the observed variation of conductivity. The whole process of charge transport in PAN, according to Mzenda et al. [7], is complex and no single model can represent it.

In this report we would like to note that the non-linearity of $I$–$V$ characteristics and its temperature behaviour, such as variation of slope with temperature and temperature dependence of energy activation, in the case of inorganic diodes can be successfully explained by addressing the phonon-assisted tunnelling as a free charge carrier generation mechanism [9, 10]. Very recently the phonon-assisted tunnelling model has been used for explanation of temperature- and field-dependent conductivity in some organic materials [11].

Therefore in this paper we present an alternative


ISSN 1648-8504

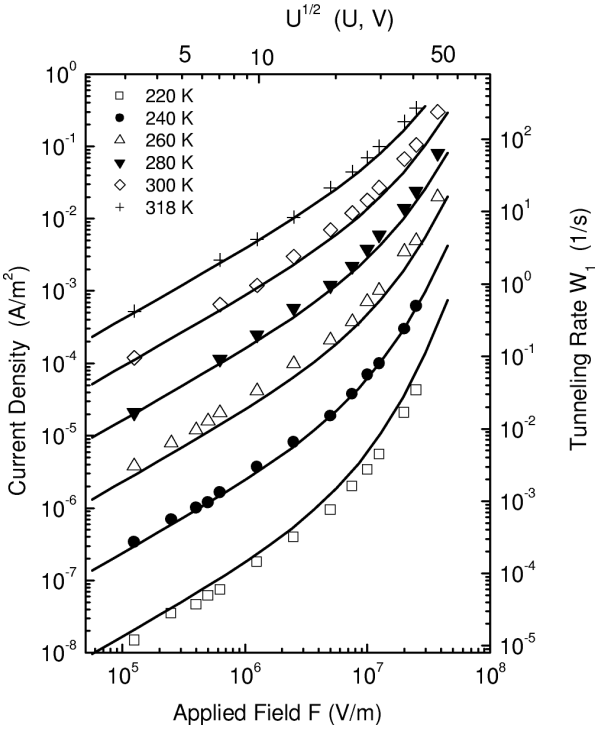


Fig. 1. $I$–$V$ characteristics of PAN films at different temperatures from Fig. 1 of Ref. [8] (symbols) fitted to the theoretical tunnelling rate $W_1(F,T)$ (solid lines) calculated at the same temperatures as the experimental data using the following parameters: $a = 11$, $\varepsilon_T = 0.6$ eV, $m^* = 2m_e$, $\hbar\omega = 12$ meV. The fit is performed under assumption that the field strength $F$ is proportional to the square root of the applied voltage.

explanation of temperature-dependent nonlinear $I$–$V$ characteristics of PAN films [8], assuming that the free charge carrier creation occurs due to the phonon-assisted tunnelling from the localized states in metal–polymer interface.

## 2. Theory and comparison of experimental data

It is assumed that the charge carriers are generated from electronic states in the polymer near the metal–polymer interface. The electrons enter the conduction band of the polymer as a result of phonon-assisted tunnelling from these levels. The filling of the electronic states at the interface is from the metal electrode. Assuming that all the released electrons are transferred through the depletion region, the current will be proportional to the tunnelling rate $W$, i. e. $I = eNWS$, where $N$ is the surface density of localized electrons, and $S$ is the area of the barrier electrode. On this basis we will compare the $I$–$V$ data extracted from Fig. 1 in Ref. [8] with the tunnelling rate $W$.

The temperature- and field-dependent tunnelling rate $W(F,T)$ was computed using the phonon-assisted

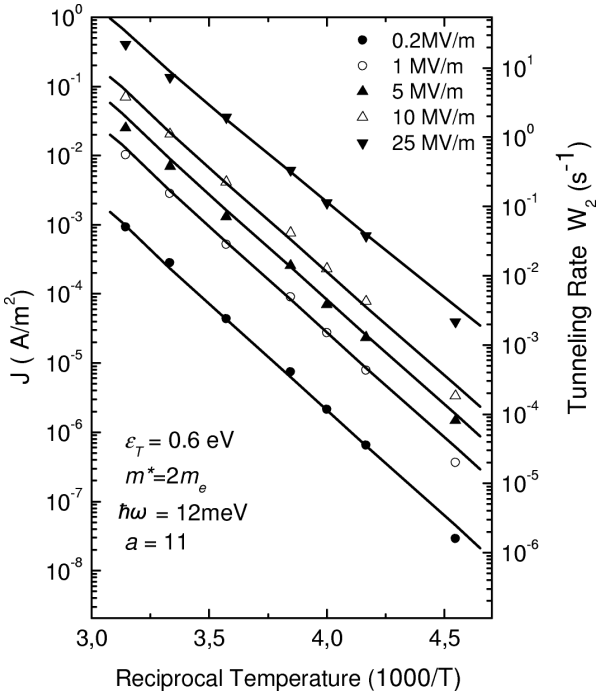


Fig. 2. Reciprocal temperature dependences of the current density at different field strengths for PAN films from Fig. 1 of Ref. [8] (symbols) fitted to the $W_1(F,T)$ dependences (solid lines) calculated for the same parameters as in Fig. 1.

tunnelling theory [12] according to the following relation:

$$W_1\ (F,T) = \frac{eF}{(8m^*\varepsilon_T)^{1/2}}[(1+\gamma^2)^{1/2}-\gamma]^{1/2}$$

$$\times(1+\gamma^2)^{-1/4}\exp\left\{-\frac{4}{3}\frac{(2m^*)^{1/2}}{eF\hbar}\varepsilon_T^{3/2}\right. \qquad (1)$$

$$\left.\times[(1+\gamma^2)^{1/2}-\gamma]^2\,[(1+\gamma^2)^{1/2}+1/(2\gamma)]\right\},$$

where

$$\gamma = \frac{(2m^*)^{1/2}\Gamma^2}{8e\hbar F\varepsilon_T^{1/2}}\,. \qquad (2)$$

Here $\Gamma^2 = 8a(\hbar\omega)^2(2n+1)$ is the width of absorption band of the centre, $n = [\exp(\hbar\omega/(k_BT))-1]^{-1}$, where $\hbar\omega$ is the phonon energy, $\varepsilon_T$ is the energetic depth of the centre, $e$ is electron charge, and $a$ is the electron–phonon interaction constant ($a = \Gamma_0^2/[8(\hbar\omega)^2]$).

The calculation was performed using the effective mass value $m^* = 2m_e$ for electron and the energy value of 12 meV for phonon. The value of activation energy $\varepsilon_T$ was determined from the plot of $\ln J$ against $1/T$ at 1 V (see Fig. 2). The electron–phonon coupling constant $a$ was chosen so as to get the best fit between the experimental data and the calculated dependences.

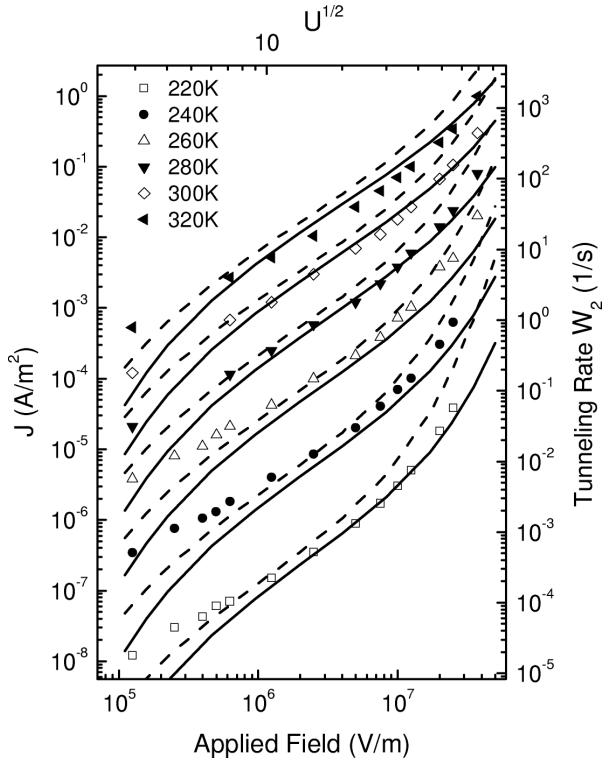


Fig. 3. The same as in Fig. 1 (symbols) but fitted to the tunnelling rate $W_2(F,T)$ dependences calculated with the following parameters: $\varepsilon_T = 0.6$ eV, $m^* = 2m_e$, $\hbar\omega = 12$ meV, $S = 22$ (solid lines). The dashed line corresponds to the tunnelling rate calculated for $m^* = m_e$.

In Fig. 1 the solid lines represent the theoretical dependences of $W_1(F,T)$ on the field strength $F$, fitted to the experimental data. The fit was performed under the assumption that the tunnelling occurs through the Schottky barrier, where the maximal field strength is proportional to the square root of the applied voltage. The comparison shows an excellent agreement of the theory with the experimental data in all the range of temperatures. From the relation $J = eNW$ the centre density $N$ close to the interface between the electrode and polymer can be estimated. From the results in Fig. 1 for $J = 10^{-7}$ Am$^{-2}$, $W$ is equal to $8{\cdot}10^{-5}$ s$^{-1}$, hence $N = 7.8{\cdot}10^{15}$ m$^{-2}$. Figure 2 illustrates $\ln J$ dependences on $1/T$ calculated for the same parameters as in Fig. 1. It can be seen that the slope of experimental curves, as well as of theoretical ones, diminishes with the increase of voltage or field strength.

We want to note that the similar temperature-dependent tunnelling rate on field strength is also given by phonon-assisted tunnelling theory developed by Makram-Ebeid and Lannoo [13]. To confirm this assertion, in Fig. 3 the comparison of the same experimental data as in Fig. 1 is shown with $W_2(F,T)$ dependences computed using the theory from [13]. The phonon-assisted tunnelling rate of electrons from the impurity centre of depth $\varepsilon_T$, derived by the use of Condon approximation, is given by the following expression (Eq. (18) in [13]):

$$W_2(F,T) = \sum_{p=-p_0}^{+p_0} RW_e(\varepsilon_T + p\hbar\omega)\,, \qquad (3)$$

where

$$R = \exp\left(\frac{p\hbar\omega}{2k_BT} - S\coth\frac{\hbar\omega}{2k_BT}\right) \times I_p\left(\frac{S}{\sinh(\hbar\omega/(2k_BT))}\right), \qquad (4)$$

$$W_e(\varepsilon_T) = \frac{2eF}{(2m^*\varepsilon_T)^{1/2}}\exp\left(-4\frac{(2m^*)^{1/2}}{3e\hbar F}\right)\varepsilon^{3/2}\,. \qquad (5)$$

Here $p_0 = \varepsilon_T/(\hbar\omega)$, $\hbar\omega$ is the phonon energy, $I_p$ is the modified Bessel function, and $S$ is the Huang–Rhys coupling constant.

The rate $W_2(F,T)$ was computed for effective mass $m^* = 2m_e$ and $S = 22$. From Fig. 3 one can see that theoretical curves also well describe the experimental results. The dashed curves represent the $W_2(F,T)$ dependences computed for the effective mass $m^* = m_e$. It is seen that in this case the theoretical curves noticeably worse describe the experimental data.

In Fig. 4 the temperature dependences of conductivity of HCl-doped PAN films from [1] and [7] fitted to $W_1(T)$ dependences are shown. It is seen that the variation of conductivity with temperature both at high and at low temperatures is well described by the variation with temperature of $W_1(T)$ alone. This circumstance strongly supports our proposed model. The deviation of experimental data from theoretical curves at temperatures lower than 50 K may be caused by the fact that at low temperatures the phonons having lower energy are more effective.

Finally, in Fig. 5 the dependences of conductivity on reciprocal temperature in the wide temperature range from 200 K to 2 K for pure PAN from Fig. 6 of [14] are shown. The experimental data were fitted to the $\ln W_2(T)$ against $1/T$ dependence computed for three values of phonon energy. The solid curve calculated for the phonon energy of 0.12 meV well matches the temperature variation of the current in low temperature region. The temperature at which the bending in these dependences occurs strongly depends on the value of phonon energy, and this allows us to estimate the energy of phonons taking part in the tunnelling process.

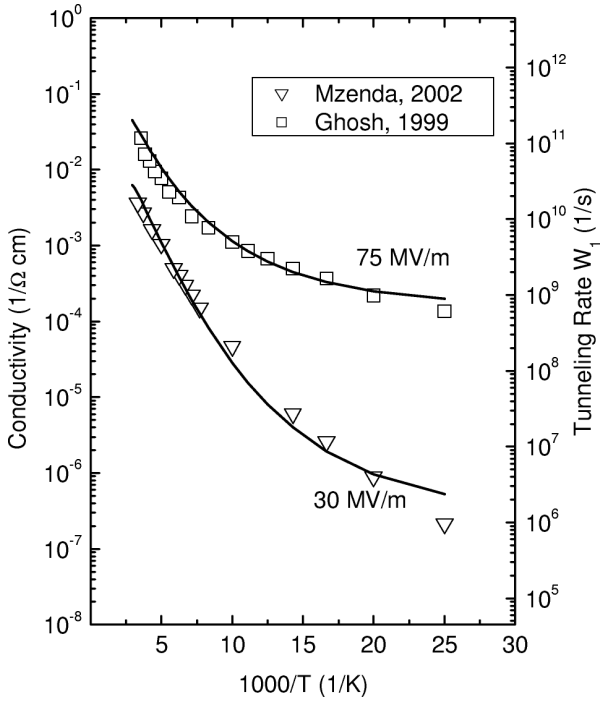


Fig. 4. Reciprocal temperature dependences of the conductivity of a PAN: from Fig. 5(a) of Ref. [1] and from Fig. 5 of Ref. [7] (symbols). The solid curves are the best fits of the data to the calculated $W_1(F,T)$ against $1/T$ dependences for the following parameters: $a = 11$, $\varepsilon_T = 0.24$ eV, $m^* = 2m_e$, $\hbar\omega = 12$ meV, and for the field strengths $F_1 = 75$ MV/m, $F_2 = 30$ MV/m.

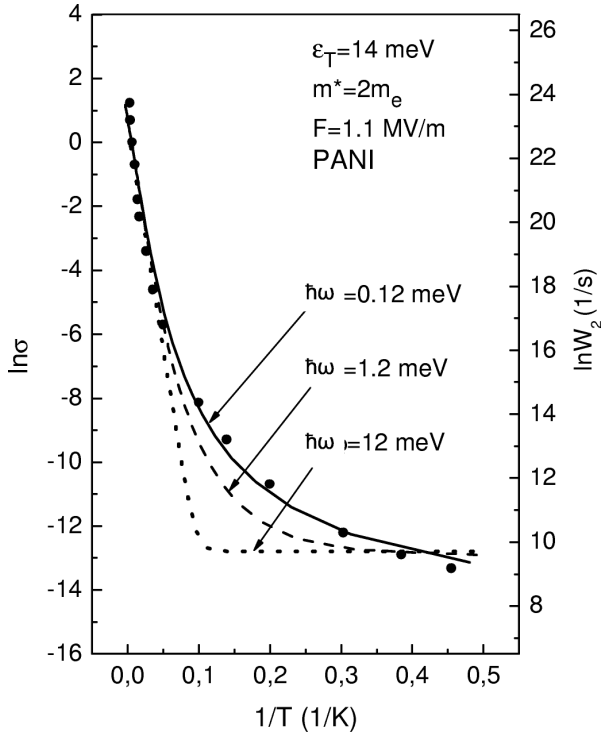


Fig. 5. Reciprocal temperature dependences of the conductivity of a pure PAN from Fig. 6 of [14] (solid circles) fitted to the tunnelling rate $W_2(F,T)$ dependences, calculated using parameters $\varepsilon_T = 14$ meV, $m^* = 2m_e$, $\hbar\omega = 0.12$ meV, $S = 30$ (solid line), $\hbar\omega = 1.2$ meV, $S = 3$ (dashed line), and $\hbar\omega = 12$ meV, $S = 1$ (dotted line).

## 3. Conclusion

In conclusion, the observed nonlinearity of $I$–$V$ characteristics of polyaniline thin films in the high field region and their variation with temperature is explained by the phonon-assisted tunnelling model proposed in [12] using Gaussian approximation for the impurity centre absorption band, as well as theory based on Condon approximation [13] and used to describe temperature behaviour of $I$–$V$ dependences in inorganic materials. From the fit of experimental $I$–$V$ dependences with the calculated $W(F)$ dependences, the density of localized states in the interface is estimated to be $\approx 10^{16}$ m$^{-2}$.

## References

[1] M. Gosh, A. Barman, A.K. Meikap, S.K. De, and S. Chatterjee, Hopping transport in HCl doped conducting polyaniline, Phys. Lett. A **260**, 138–148 (1999).

[2] A.J. Epstein, J.M. Ginder, F. Zuo, R.W. Bigelow, H.-S. Woo, D.B. Tanner, A.F. Richter, W.-S. Huang, and A.G. MacDiarmid, Insulator-to-metal transition in polyaniline, Synth. Met. **18**, 303–309 (1987).

[3] Z.H. Wang, E.M. Scherr, A.G. MacDiarmid, and A.J. Epstein, Transport and EPR studies of polyaniline: A quasi-one-dimensional conductor with three-dimensional "metallic" states, Phys. Rev. B **45**, 4190–4202 (1992).

[4] M. Reghu, Y. Cao, D. Moses, and A.J. Heeger, Counterion-induced processibility of polyaniline: Transport at the metal–insulator boundary, Phys. Rev. B **47**, 1758–1764 (1993).

[5] R. Menon, C.O. Yoon, D. Moses, and A.J. Heeger, Transport in polyaniline near the critical regime of the metal–insulator transition, Phys. Rev. B **48**, 17685–17694 (1993).

[6] R. Pelster, G. Nimtz, and B. Wessling, Fully protonated polyaniline: Hopping transport on a mesoscopic scale, Phys.Rev. B **49**, 12718–12723 (1994).

[7] V.M. Mzenda, S.A. Goodman, and F.D. Auret, Conduction models in polyaniline: The effect of temperature on the current–voltage properties of polyaniline over the temperature range 30 < T(K) < 300, Synth. Met. **127**, 285–289 (2002).

[8] Y. Kieffel, J.-P. Travers, and J. Planes, Nonlinear electrical properties of polyaniline: Role of conjugation length, Synth. Met. **135–136**, 325–326 (2003).

[9] P.A. Pipinis, A.K. Rimeika, and V.A. Lapeika, Temperature dependence of the reverse current in Schottky barrier diodes, Semiconductors **32**(7), 785–788 (1998).
[10] P. Pipinys, A. Pipiniene, and A. Rimeika, Phonon-assisted tunneling in reverse biased Schottky diodes, J. Appl. Phys. **86**(12), 6875–6878 (1999).
[11] P. Pipinys, A. Rimeika, and V. Lapeika, DC conduction in polymers under high electric fields, J. Phys D. 37, 828–831 (2004).
[12] A. Kiveris, Š. Kudžmauskas, and P. Pipinys, Release of electrons from traps by an electric field with phonon participation, Phys. Status Solidi A **37**, 321–327 (1976).
[13] S. Makram-Ebeid and M. Lannoo, Quantum model for phonon-assisted tunnel ionization of deep levels in a semiconductor, Phys. Rev. B **25**, 6406–6424 (1982).
[14] W.K. Maser, A.M. Benito, M.A. Callejas, T. Seeger, M.T. Martinez, J. Schreiber, J. Muszynski, O. Chauvet, Z. Osváth, A.A. Koós, and L.P. Biró, Synthesis and characterization of new polyaniline/nanotube composites, Mat. Sci. Engin. C **23**, 87–91 (2003).

## POLIANILINO VOLTAMPERINIŲ PRIKLAUSOMYBIŲ NETIESIŠKUMAS FONONAIS PASKATINTŲ TUNELINIŲ ŠUOLIŲ POŽIŪRIU

A. Kiveris, P. Pipinys

*Vilniaus pedagoginis universitetas, Vilnius, Lietuva*

**Santrauka**

Netiesinės polianilino plonų plėvelių voltamperinių charakteristikų temperatūrinės priklausomybės (eksperimentiniai autorių duomenys iš [1, 7, 8, 14]) palygintos su teorinėmis krūvininkų tunelinių šuolių dalyvaujant fononams tikimybių priklausomybėmis nuo temperatūros ir elektrinio lauko stiprio. Eksperimento duomenys gerai atitinka apskaičiuotas tuneliavimo spartos priklausomybes nuo lauko stiprio ir temperatūros. Palyginus eksperimentinius duomenis su teorinėmis priklausomybėmis rastas paviršinis srovę sąlygojančių lokalizuotų centrų tankis, lygus $\approx 10^{16}$ m$^{-2}$.